ISA Transactions ■ (■■■■) ■■■–■■■

Contents lists available at ScienceDirect

ISA Transactions

journal homepage: www.elsevier.com/locate/isatrans

Fault diagnosis method based on FFT-RPCA-SVM for Cascaded-Multilevel Inverter

Tianzhen Wang [a,*,1], Jie Qi [a], Hao Xu [a], Yide Wang [b], Lei Liu [a], Diju Gao [a]

[a] Shanghai Maritime University, China
[b] Ecole polytechnique Université de Nantes, L'Institut d'Electronique et de Télécommunications de Rennes, UMR CNRS 6164, France

ARTICLE INFO

Article history:
Received 20 March 2015
Received in revised form
9 October 2015
Accepted 12 November 2015

Keywords:
Fault diagnosis
Fast Fourier Transform
Relative principal component analysis
Support Vector Machine
Cascaded-Multilevel Inverter
Wind turbine

ABSTRACT

Thanks to reduced switch stress, high quality of load wave, easy packaging and good extensibility, the cascaded H-bridge multilevel inverter is widely used in wind power system. To guarantee stable operation of system, a new fault diagnosis method, based on Fast Fourier Transform (FFT), Relative Principle Component Analysis (RPCA) and Support Vector Machine (SVM), is proposed for H-bridge multilevel inverter. To avoid the influence of load variation on fault diagnosis, the output voltages of the inverter is chosen as the fault characteristic signals. To shorten the time of diagnosis and improve the diagnostic accuracy, the main features of the fault characteristic signals are extracted by FFT. To further reduce the training time of SVM, the feature vector is reduced based on RPCA that can get a lower dimensional feature space. The fault classifier is constructed via SVM. An experimental prototype of the inverter is built to test the proposed method. Compared to other fault diagnosis methods, the experimental results demonstrate the high accuracy and efficiency of the proposed method.

1. Introduction

With global expansion of economy, the demand for energy from all walks of life is increasing year by year. Countries in the world therefore try to explore every possible energy resource. The exploitation of renewable resources has become an international hot spot. Inverter system is a key part of renewable resources exploitation which converts DC to AC. Multilevel inverter is suitable for applications in the direct drive wind power system because it can reduce the switch voltage stress and the equivalent switching frequency. In recent years, cascaded H-bridge multilevel inverter system (CHMLIS), as a kind of multi-level inverter with good implementation properties, is widely used in high-power transform domain. It is used namely in the direct drive wind power system, which adopts a low-speed multi-phase permanent magnet synchronous generator. CHMLIS offers many advantages for high-voltage or high-power applications. However, with increasing number of levels, the probability of faults in wind power system will increase, such as open-circuit (OC) or short-circuit (SC) of the power switch transistors [1–3], which will cause the shutout of the wind power system or some catastrophic accidents. In order to guarantee normal operation of wind power system, the research on cascaded H-bridge multi-level inverter fault diagnosis has important theoretical significance and application values [4,5]. The faults of inverter, mainly composed of power switch transistors, are OC or SC [1–3,6]. For different fault types and locations, the system's voltage and current will be different. In order to achieve the purpose of quickly and effectively detecting the faults and estimating their type and location, the researchers usually combine a variety of fault diagnosis methods applied to the system current or voltage variation [7–10]. Several diagnosis approaches for inverter have been presented in [11–13]. But they have some problems such as nonlinear factors in the multilevel inverter and the complex circuit configuration. In [14], a novel approach based on an adaptive kernel principal component analysis and Support Vector Machine (SVM) is proposed for real-time fault diagnosis of high-voltage circuit breakers. SVM is powerful for small sample data classification, but the generalization ability of SVM will be decreased for large classification. A diagnosis approach using neural networks is proposed in [15] for fault identification using partial syndromes. Neural networks have strong nonlinear fitting capability, but the learning speed of ANN is rather slow. In [16], a multilevel principal component analysis based fault diagnosis method is proposed to provide meaningful monitoring of the underlying process and help faults diagnosis. However, multilevel principal component analysis is more powerful in fault detection than in fault diagnosis. Another fault diagnosis method based on the normalized DC current is

* Correspondence to: Department of Electrical Automation, Shanghai Maritime University, Shanghai, China. Tel.: +86 21 38282640.
E-mail address: wtz0@sina.com (T. Wang).
[1] Permanent address: Department of Electrical Automation, College of Logistics Engineering, Shanghai Maritime University, Shanghai 201306, China.

http://dx.doi.org/10.1016/j.isatra.2015.11.018
0019-0578/

presented in [17] for voltage source active rectifiers and in [18] for voltage source inverter. But, the output current of CHMLIS depends on the load variation, which leads to a false diagnosis when the load changes. In [19], a smart diagnosis method based on multi-kernel support vector machines and incremental learning is proposed to achieve accurate faulty-component classification based on observed errors. However, when the sample data or fault classes are big, the running time will be increased greatly. A sensor fault diagnosis approach is presented based on principle component analysis (PCA) feature extraction and SVM multi-classification in [20]. An approach based on lifting wavelet transform and SVM is proposed in [21] to improve the accuracy of fault identification. An imbalanced pattern classification method, based on under-sampling, for SVM is proposed in [22]. [23] proposes a control chart pattern recognition method based on genetic algorithm and PCA-SVM. However, the accuracy and efficiency of diagnosis should be improved due to the lack of data preprocessing. The method proposed in [1], can handle large transients such as load and speed variations, without emitting false diagnostics. However, this approach requires complex pattern recognition algorithms which are not easy to be integrated into the drive controller. The algorithm proposed in [24] detects effectively the inverter faulty phase, is capable of localizing the faulty power switch, and avoids the use of extra sensors or electrical devices and the subsequent increase of system complexity and costs. However, it can be observed that, for the case of open circuit faults, due to the specific features of power inverter topology, it is possible that a faulty insulated-gate bipolar transistor would not be localized if the failure occurs during the phase of demagnetization.

This paper proposes a cascaded multi-level inverter fault diagnosis strategy, which includes two parts. One is the test signals selection of CHMLIS: by the contrast analysis of the inverter output voltage and current signals when the switch transistors are in open circuit state, the output voltage signals have been chosen as the fault characteristic signals. The other is the proposed FFT-RPCA-SVM method. SVM is not good for large sample classification. So, FFT is used to preprocess the original signals to do data compression and feature extraction. And the relative principal component analysis (RPCA) is used to make data optimization and dimension reduction. Finally SVM is adopted to realize the faults classification. In order to obtain simulation data, a CHMLIS simulation model is constructed. In addition, a CHMLIS fault diagnosis experiment platform is constructed, which is based on dSPACE real-time system, to get experimental data. For verifying the effectiveness of the proposed method, the proposed technique and other traditional fault diagnosis methods are compared with the simulated and experimental data. The results show that the proposed fault diagnosis strategy improves the diagnosis accuracy and computational efficiency.

2. Signals selection of CHMLIS

CHMLIS is used in direct drive wind power system as shown in Fig. 1. Because the topology of every phase is the same, a single-phase cascaded H-bridge five-level inverter switch transistors in open-circuit (OC) is taken as an example (Fig. 2). OC fault means that the power semiconductor device remains in off-state permanently. Mostly OC fault appears when the gate driver unit or the gate firing hardware circuit fails [22]. This cascaded H-bridge five-level inverter simulation model is controlled by Subharmonic PWM (SHPWM) [30,31], the output voltage is obtained via an amplitude modulated wave with modulation ratio m_a. When $m_a=0.86$, the single-phase five-level inverter circuit output voltage and current waveforms are shown in Fig. 3. The inverter normal state's output waveforms with load resistance $R_{load}=1\ k\Omega$ are shown in Fig. 3(a). As shown in Fig. 3(a), the output voltage and current waveforms have the same shape; the proportionality between the waveforms is the load resistance. Fig. 3(b) and (c) shows the single-phase five-level inverter output voltage and current waveforms when the H-bridge S1 switch transistor is in OC fault with load resistance $R_{load}=1\ k\Omega$ and $100\ \Omega$, respectively. It can be observed through analyzing Fig. 3(b) and (c), that the output voltage values remain constant with the change of the inverter load, but the output current waveforms change with the load variation. It can then be concluded, that the output current depends on the load variation, but the inverter output voltage is independent of the load variation, and the output voltage waveforms are different for different locations of switch OC faults as shown in Fig. 4.

It is very important to select the appropriate signals, for fault detection and diagnosis, which will directly affect the diagnostic performance. It can be observed from the above analysis, that the output current depends on the load variation, which will lead to a false diagnosis when the load changes. Therefore, it is inappropriate to only employ the output current waveforms as the model characteristic signals. The output voltage waveforms have the following merits: 1) less additional circuit where only a voltage detecting sensor at the inverter output terminal is sufficient; 2) the inverter output voltage does not change with the load variation; 3) the inverter output voltage changes with different faults; 4) simple calculation because only the inverter output voltage is used to locate the faults. Therefore the output voltage signals of CHMLIS are selected as the input fault classification characteristic signals for the fault diagnosis method in this paper.

A single-phase cascaded five-level inverter including H-bridge1 and H-bridge2 is shown in Fig. 2. Every switch may have open circuit fault, and the normal state is also listed as a special class of faults, generally there are 9 kinds of fault categories in single-phase cascaded H-bridge five-level inverter. The category labels are used to represent fault category as shown in Table 1. When a fault signal belongs to a fault category, the corresponding fault classification

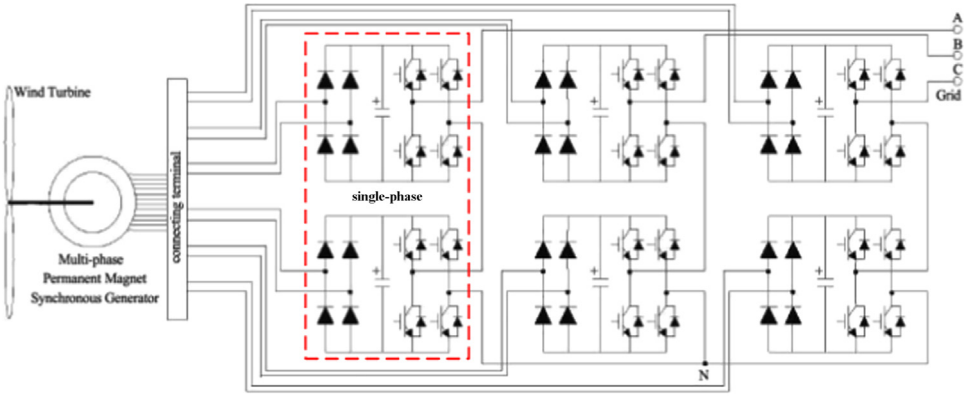

Fig. 1. Direct drive wind power system of cascade H-bridge five-level inverter.

Please cite this article as: Wang T, et al. Fault diagnosis method based on FFT-RPCA-SVM for Cascaded-Multilevel Inverter. ISA Transactions (2015), http://dx.doi.org/10.1016/j.isatra.2015.11.018

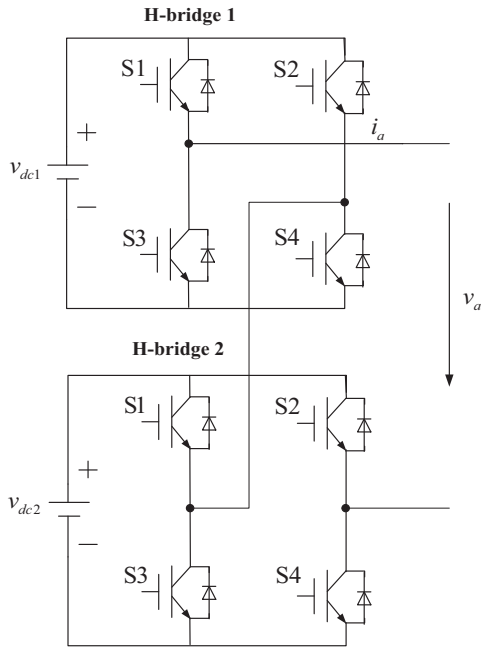

Fig. 2. Single-phase cascaded five-level inverter.

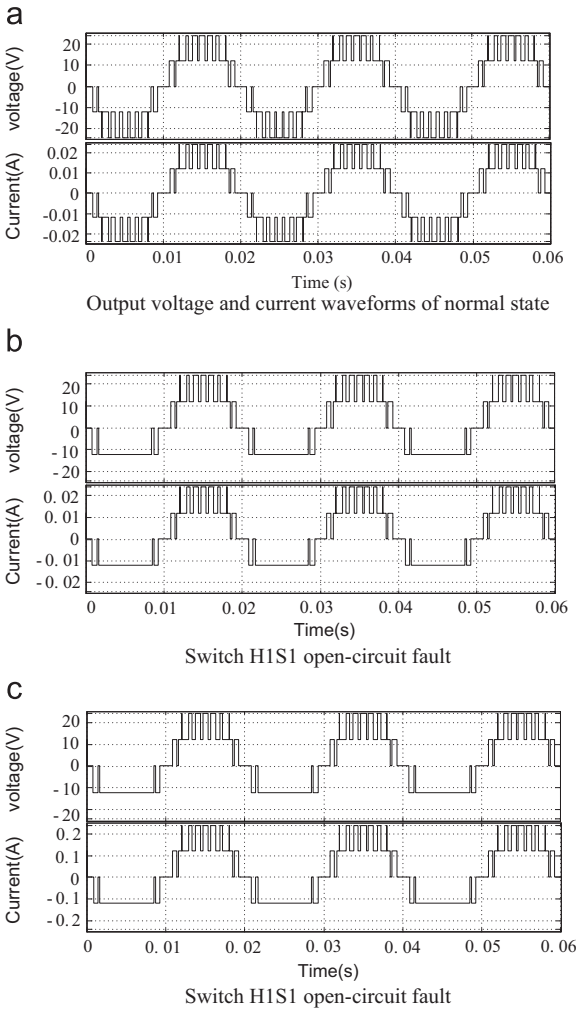

Fig. 3. Output voltage and current waveforms. (a) Output voltage and current waveforms of normal state, (b) switch H1S1 open-circuit fault and (c) switch H1S1 open-circuit fault.

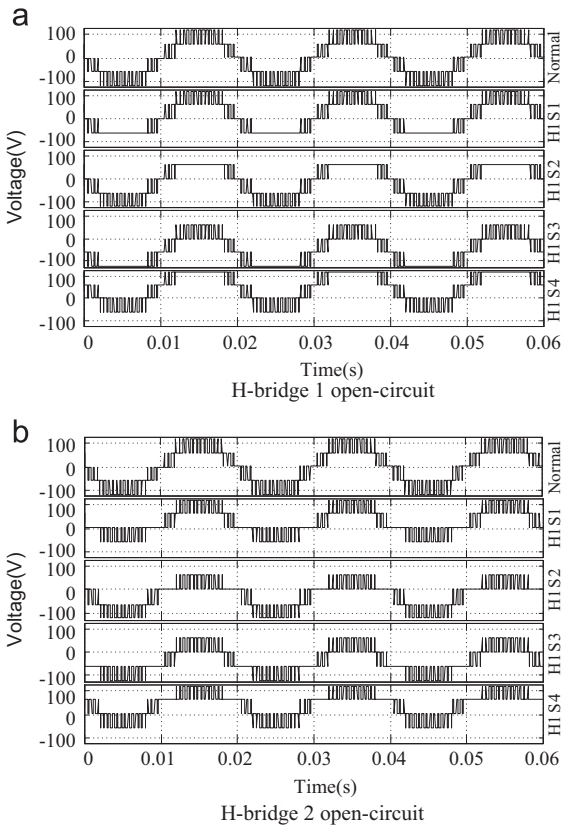

Fig. 4. Output waveforms when Cascaded H-bridge switch S1-S4 open-circuit. (a) H-bridge 1 open-circuit and (b) H-bridge 2 open-circuit.

Table 1
Fault and category labels.

No.	Fault	Category labels
1	Normal	[1, 0, 0, 0, 0, 0, 0, 0, 0]^T
2	H1S1 Open	[0, 1, 0, 0, 0, 0, 0, 0, 0]^T
3	H1S2 Open	[0, 0, 1, 0, 0, 0, 0, 0, 0]^T
4	H1S3 Open	[0, 0, 0, 1, 0, 0, 0, 0, 0]^T
5	H1S4 Open	[0, 0, 0, 0, 1, 0, 0, 0, 0]^T
6	H2S1 Open	[0, 0, 0, 0, 0, 1, 0, 0, 0]^T
7	H2S2 Open	[0, 0, 0, 0, 0, 0, 1, 0, 0]^T
8	H2S3 Open	[0, 0, 0, 0, 0, 0, 0, 1, 0]^T
9	H2S4 Open	[0, 0, 0, 0, 0, 0, 0, 0, 1]^T

category is labeled 1, the other categories are labeled 0, so every fault could be distinguished easily. The output vector index set is recorded as I={normal, H1S1, H1S2, H1S3, H1S4, H2S1, H2S2, H2S3, H2S4}.

3. FFT-RPCA-SVM fault diagnosis method

According to the above analysis about the signals of CHMLIS, the key problems are the efficiency and accuracy for fault diagnosis. The structure of FFT-RPCA-SVM fault diagnosis method is shown in Fig. 5, where the CHMLIS fault diagnosis can be divided into four parts: voltage signal pre-processing, classification diagnosis, output diagnostic results and switching model calculation. And this paper mainly considers the first three parts.

3.1. Signal preprocessing based on FFT

Each fault has its own unique frequency signature [27,28]. And it is difficult for SVM to use the large sample directly for fault

Please cite this article as: Wang T, et al. Fault diagnosis method based on FFT-RPCA-SVM for Cascaded-Multilevel Inverter. ISA Transactions (2015), http://dx.doi.org/10.1016/j.isatra.2015.11.018

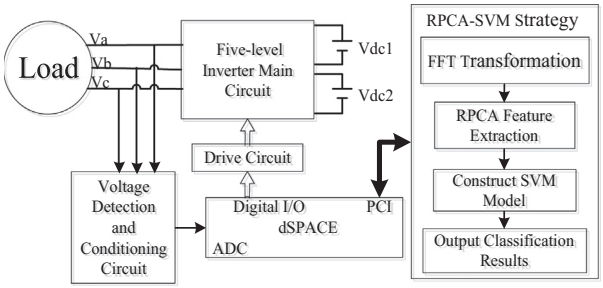

Fig. 5. Structure of fault diagnosis method.

classification. So, FFT is used to process output voltage signals and the first b (b < < number of samples) frequencies are used for the feature data for next step (RPCA), which will improve the diagnosis accuracy and computational efficiency of CHMLIS.

For a sequences of discrete output voltage signal $\mathbf{X}_{a\times N}(i,n)=f_{i,n}$, with $i=1, 2, \ldots, a$, and $n=0, 1, 2, \ldots N-1$, the resulted reduced data $\overline{\mathbf{X}}_{a\times b}(i,k)=F_{i,k}$, with $i=1,2,\ldots,a$, and $k=0,1,2,\ldots b-1$ could be got after FFT transformation, where a is the size of training samples or test samples, b is the size of the retained harmonics [28]. FFT transformation is shown in Eqs. (1) and (2).

$$F_{i,\,k}=G_{i,k}+W_N^k H_{i,k} \tag{1}$$

$$F_{i,\,k+N/2}=G_{i,\,k}-W_N^k H_{i,k} \tag{2}$$

where $W_N=e^{-j2\pi/N}$, N is the number of sampling points in discrete output voltage signal, $k=0,\ldots,\frac{N}{2}-1$. $G_{i,k}$ and $H_{i,k}$ can be calculated by (3) and (4).

$$G_{i,k}=\sum_{n=0}^{(N/2)-1} f_{i,2n}W_{N/2}^{nk} \tag{3}$$

$$H_{i,k}=\sum_{n=0}^{(N/2)-1} f_{i,2n+1}W_{N/2}^{nk} \tag{4}$$

3.2. Feature extraction based on RPCA

After FFT, the first b (b«number of samples) frequencies are kept. However, the dimension of variables is still high. RPCA is then used to remove the correlation between variables and reduce the dimension of variables, and therefore to extract the most significant components though weighting different variables by **M**.

RPCA is used to extract more effective principal components [29]. Firstly, the data after FFT are normalized by (5) to remove the mean value in the samples and to facilitate the RPCA process. Secondly, according to the prior knowledge, the relative importance of different variables is analyzed. For example, the first 40 frequencies are much more important than others in CHMLIS fault diagnosis after FFT. And then all the variables are weighted by (6).

$$\mathbf{X}^*=\frac{\overline{\mathbf{X}}_{a\times b}-E(\overline{\mathbf{X}}_{a\times b})}{\mathrm{Var}(\overline{\mathbf{X}}_{a\times b})^{1/2}} \tag{5}$$

$$\mathbf{X}^R=\mathbf{X}^*\times\mathbf{M} \tag{6}$$

where $\mathbf{X}^*$ is the normalized sample matrix, $\mathrm{E}(\overline{\mathrm{X}}_{a\times b})$ is the mean of $\overline{\mathrm{X}}_{a\times b}$, $\mathrm{Var}(\overline{\mathrm{X}}_{a\times b})^{1/2}$ is the standard deviation of $\overline{\mathrm{X}}_{a\times b}$, X^R is an a × b matrix, $\mathbf{M}=\mathbf{diag}(M_1,M_2,\ldots,M_b)$ is the relative weighting operator, **M** is set according to the relative importance of different variables [25,26]. When =**I**, RPCA is equivalent to PCA. So, **M** is useful to take the relative importance of variables into account. In order to get the principal components (PCs) of $\mathbf{X}^R$, the correlation matrix (or covariance matrix, because the mean value of X^R is zero) equation can be calculated from (7)

$$\Sigma_{\mathbf{X}^R}=\mathrm{E}\left\{\left[\mathbf{X}^R\right]^{\mathrm{T}}\left[\mathbf{X}^R\right]\right\} \tag{7}$$

The eigenvalues λ^R and the corresponding eigenvectors $\mathbf{e}^R$ can be obtained by (8) and (9).

$$\left|\lambda^R\mathbf{I}-\Sigma_{\mathbf{X}^R}\right|=0 \tag{8}$$

$$\left[\lambda_i^R\mathbf{I}-\Sigma_{\mathbf{X}^R}\right]\mathbf{e}_i^R=0,\ i=1,2,\ldots,b \tag{9}$$

where λ_i^R is the ith eigenvalue, and is arranged decreasing order as $\lambda_1^R\geq\lambda_2^R\geq\cdots\geq\lambda_b^R$, $\mathbf{e}_i^R$ is the eigenvector corresponding to λ_i^R, $\mathbf{e}_i^R=\left[\boldsymbol{e}_i^R(1),\boldsymbol{e}_i^R(2),\cdots,\boldsymbol{e}_i^R(b)\right]^{\mathrm{T}}$.

Finally, a new lower dimensional matrix $\mathbf{T}_{a\times m}$ can be calculated from (10)

$$\mathbf{T}=\boldsymbol{X}_{a\times b}\times\boldsymbol{E}_{b\times m} \tag{10}$$

where **T** is an $a\times m$ matrix, $\mathbf{E}_{b\times m}=[\mathbf{e}_1^R,\mathbf{e}_2^R,\ldots,\mathbf{e}_m^R]$. m is the size of PCs, which is selected by (11).

$$CPV(m)=\frac{\Sigma_1^m\lambda_i^R}{\Sigma_1^b\lambda_i^R}\times 100\%>P \tag{11}$$

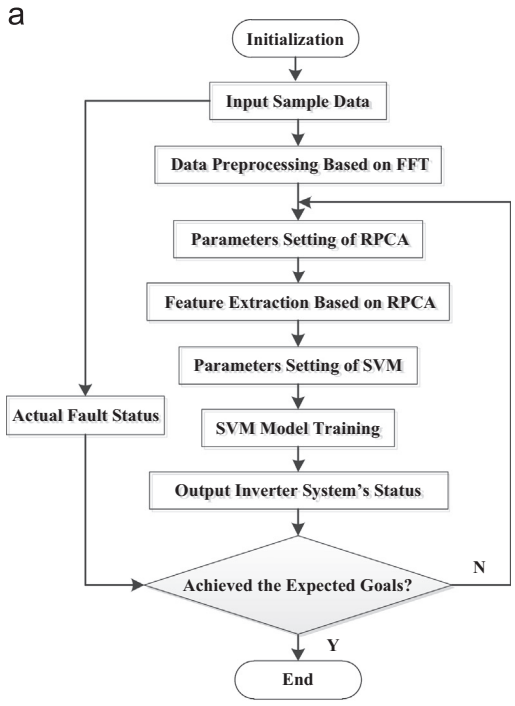

FFT-RPCA-SVM method training process

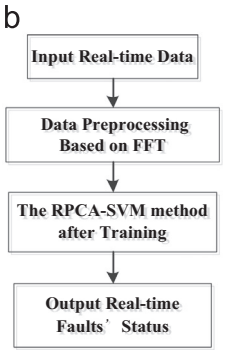

Real-time online fault diagnosis

Fig. 6. Flow chart of fault diagnosis method based on the FFT-RPCA-SVM. (a) FFT-RPCA-SVM method training process and (b) real-time online fault diagnosis.

Please cite this article as: Wang T, et al. Fault diagnosis method based on FFT-RPCA-SVM for Cascaded-Multilevel Inverter. ISA Transactions (2015), http://dx.doi.org/10.1016/j.isatra.2015.11.018

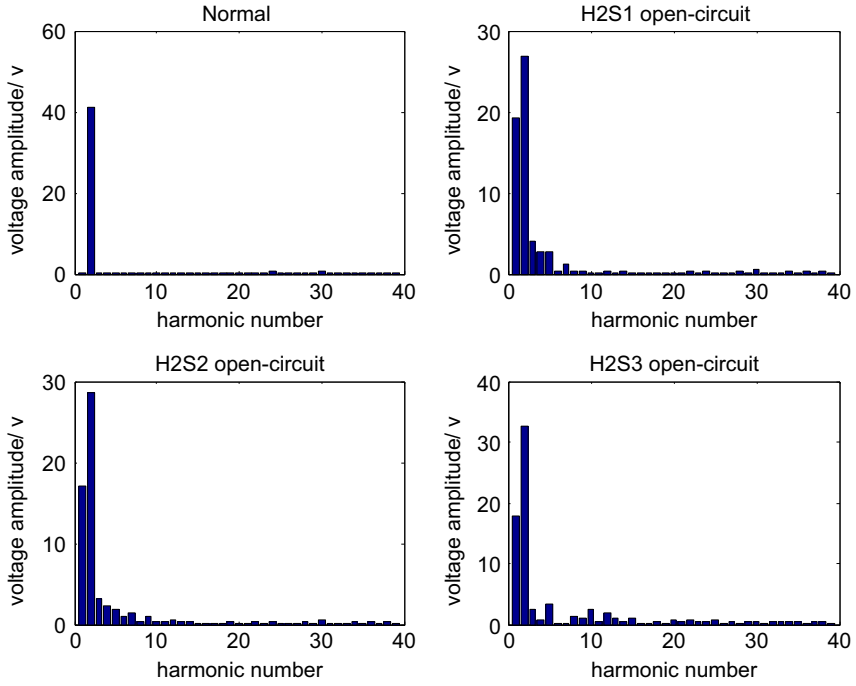

Fig. 7. Harmonics amplitude after FFT.

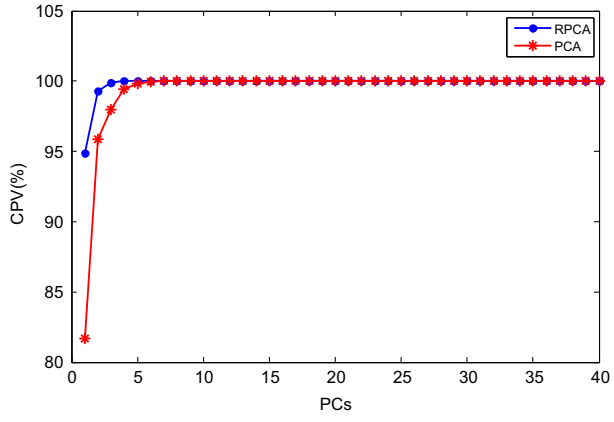

Fig. 8. *CPV* with size of the first PCs.

The value of P can be determined by the user as a predetermined threshold.

3.3. Fault classification diagnosis based on SVM

Suppose that there are L sub-networks in SVM. L is the total number of fault types. $\mathbf{T}$ is the input data of SVM which is divided into two parts, one part is $\mathbf{T}_{\text{train}}$, the other part is $\mathbf{T}_{\text{test}}$. According to Table 1, each target output value of SVM sub-network is either 0 or 1, i.e., when the target belongs to the ith SVM sub-network, the ith sub-network output is labeled 1 and the other sub-networks are labeled 0. The appropriate kernel function and the penalty factor $\mathbf{C}$ can be selected after training and testing SVM with training set $[\mathbf{T}_{\text{train}}, \mathbf{t}_{\text{train}}]$ and testing set $[\mathbf{T}_{\text{test}}, \mathbf{t}_{\text{test}}]$ [30]. And the diagnosis accuracy of SVM can be obtained through the comparison of the test output with the actual output. The fault diagnosis flowchart of the proposed FFT-RPCA-SVM method is shown in Fig. 6. The FFT-RPCA-SVM method training process is shown in Fig. 6(a). It can be described as follows. Firstly, preprocess the sampled data based on FFT. Secondly, find the most significant parameters by RPCA. Thirdly, set the SVM parameters and train the SVM model. Finally, output the status if the results achieve the expected goals, or go to the second step. Fig. 6(b) shows the real-time online fault diagnosis of the FFT-RPCA-SVM method after training.

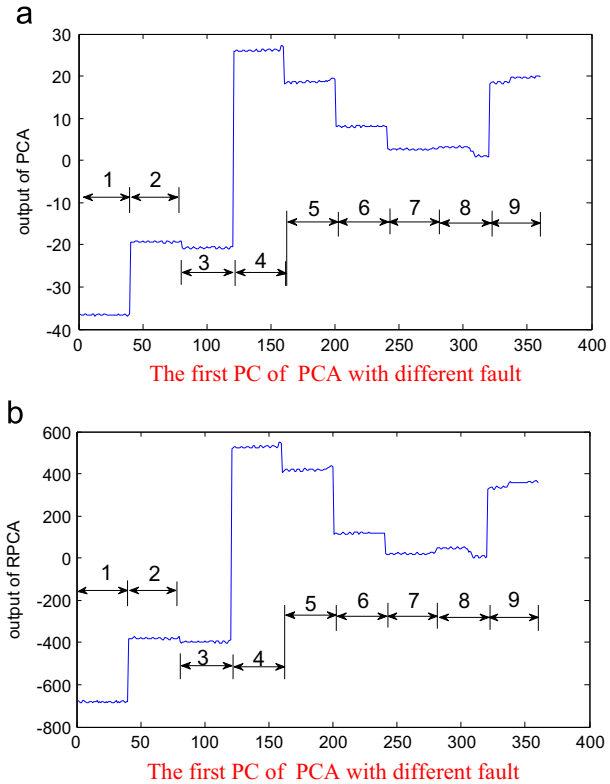

Fig. 9. The first PC of PCA and RPCA with different fault. (a) The first PC of PCA with different fault and (b) the first PC of RPCA with different fault.

Please cite this article as: Wang T, et al. Fault diagnosis method based on FFT-RPCA-SVM for Cascaded-Multilevel Inverter. ISA Transactions (2015), http://dx.doi.org/10.1016/j.isatra.2015.11.018

4. Simulation results and analysis

In order to verify the effectiveness and diagnostic performance of the proposed method, the experiments are tested on the simulation model of a single-phase five-level cascaded H-bridge inverter described in Section 2. The output voltage signals of inverter under various situations are selected as the simulation data. In order to test the fault diagnosis performance of the proposed FFT-RPCA-SVM method, the parameters are set as follows, the adjustable amplitude modulation ratio m_a is set from 0.5 to 1, the sampling frequency f is 50 kHz, the measuring time is 0.2 s in each simulation, so the sampling number N is 1000. The sampled output voltage signals are converted into 0–39 harmonics by FFT, where 0 means the DC component of the output voltage signals. After many tests, we find that the first 40 harmonics are enough to meet the demand for fault diagnosis accuracy.

4.1. Fault diagnosis based on FFT-RPCA-SVM method

FFT is used to achieve signal preprocessing after getting voltage signal from the inverter. Because comparing with the voltage signal shown in Fig. 4, it is much easier to distinguish the faults by using the spectrum shown in Fig. 7.

As shown in Fig. 8, the first PC of PCA contains 82% of the total energy. However, the first PC of RPCA contains almost 94% of the total energy when $\mathbf{M}=\{M_1=20,\ M_2=M_3=M_4=10,\ M_i=1|i=5,\ 6,\ \ldots,\ 40\}$. So, the feature information from the first PC of RPCA is more than from the first PC of PCA.

Fig. 9 shows the first PC of PCA and RPCA with different fault, where each fault contains 40 sets of samples. '1, 2, 3…' mean the category labels of different faults from Table 1. It is difficult to distinguish fault 7 and fault 8 by the first PC of PCA as shown in Fig. 9(a). However, RPCA can do this much easier as shown in Fig. 9 (b). RBF kernel is selected as the kernel function of SVM [31].

Table 2
Parameters configuration for different methods.

Methods	Parameter configuration
FFT-BP	$innum=2, midnum=8, outnum=9, f(x)=\frac{1}{1+e^{-x}}, \eta=0.01.$
FFT-SVM	$\mathbf{K}(x,y)=\exp(-\gamma\|x-y\|^2),\ c=5,\ \gamma=1/9$
FFT-PCA-SVM	$\mathbf{K}(x,y)=\exp(-\gamma\|x-y\|^2),\ c=5, \gamma=1/9$
FFT-RPCA-SVM	$\mathbf{M}=\{M_1=20,\ M_2=M_3=M_4=10,\ M_i=1\|i=5,\ 6,\ \ldots,\ 40\}$, $\mathbf{K}(x,y)=\exp(-\gamma\|x-y\|^2),\ c=5, \gamma=1/9$

4.2. Comparison and analysis

In order to verify the effectiveness of the proposed FFT-RPCA-SVM method, FFT-BP, FFT-SVM and FFT-PCA-SVM are compared with the proposed FFT-RPCA-SVM method in the simulation test. The Parameters Configuration for different methods is shown in Table 2. There are 162 training samples which are randomly selected from 315 history samples with a 10% white Gaussian noise, and the testing data are randomly selected with size of 45, 72, 108 and 153 samples from the remaining (315–162=153) samples. Each method is running 50 times corresponding to each test data set, respectively. The average fault diagnosis results of these methods are shown in Table 2.

According to Table 3, the average diagnostic accuracy rate of FFT-BP is around 70%, with a rather long running time. The diagnostic accuracy rate of FFT-SVM is about 94% with running time much shorter than that of FFT-BP algorithm. The running time of FFT-PCA-SVM and FFT-RPCA-SVM is almost the same. FFT-RPCA-SVM method reaches the highest accuracy rate which is 100%. The diagnostic accuracy of FFT-RPCA-SVM is better than FFT-PCA-SVM. The main reason is that the first PCs of RPCA contains more information of the data after FFT. Compared with FFT-BP, FFT-SVM and FFT-PCA-SVM, the proposed method is able to greatly reduce the running time, and improve the diagnostic accuracy. The simulation results have achieved the expected goals and verified the effectiveness of the FFT-RPCA-SVM method.

5. Application in CHMLIS

The proposed method is tested with a cascaded H-bridge multilevel inverter fault diagnosis experimental platform which has

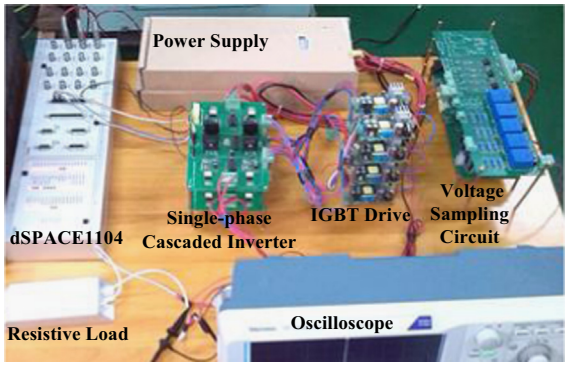

Fig. 10. Experimental platform of cascaded H-bridge inverter.

Table 3
Diagnostic results of four methods.

Different methods			Test samples			
			45 groups	72 groups	108 groups	153 groups
Running time (ms)	FFT-BP		1629	1248	634	1306
	FFT-SVM		29.8	28.6	42.5	58.0
	FFT-PCA-SVM PCs=1		8.6	10.2	10.1	12.1
	FFT-RPCA-SVM PCs=1		8.7	10.4	10.6	12.4
Diagnostic accuracy (%)	FFT-BP		71.8	71.3	72.7	67.4
	FFT-SVM		94.1	94.3	92.0	92.5
	FFT -PCA -SVM	PCs=4	100	98.3	97.3	96.3
		PCs=1	92.5	90.4	89.7	88.9
	FFT -RPCA -SVM	PCs=4	100	100	100	100
		PCs=1	100	100	100	100

Please cite this article as: Wang T, et al. Fault diagnosis method based on FFT-RPCA-SVM for Cascaded-Multilevel Inverter. ISA Transactions (2015), http://dx.doi.org/10.1016/j.isatra.2015.11.018

Table 4
Results based on four methods.

Different methods			Test samples			
			45 groups	72 groups	108 groups	153 groups
Running time (ms)	FFT-BP		1617	1541	710	1677
	FFT-SVM		27.5	28.1	42.4	58.3
	FFT-PCA-SVM PCs=1		9.8	10.7	12.1	13.1
	FFT-RPCA-SVM PCs=1		9.9	11.1	12.0	13.7
Diagnostic accuracy (%)	FFT-BP		70.3	69.8	73.4	68.8
	FFT-SVM		96.0	94.0	91.9	90.6
	FFT -PCA	PCs=4	100	97.2	96.5	95.5
	-SVM	PCs=1	91.1	89.8	88.9	88.1
	FFT -RPCA	PCs=4	100	100	100	100
	-SVM	PCs=1	100	100	100	100

been built based on dSPACE1104 platform as shown in Fig. 10, wherein the inverter hardware circuit includes a dead-zone circuit, a driving circuit consisting of integrated power modules TLP250 and an H-bridge main circuit. N-channel power IGBTIRGP35B60PD is selected as the power switch transistors in this system, which includes a built-in reverse diode. S-35-12 is selected as switch power with input 115–230 V/AC and output +12 V.

The voltage signals at different operating point can be obtained via the hardware circuit experiments with $0.8 \leq ma \leq 0.95$. There are 315 data samples after FFT transform, among which 162 are used as training data, and the remaining 153 are taken as testing data. The sample fault type labels are set according to Table 1. The other parameters are set as the same as in the above simulation test.

In order to show the effectiveness of the proposed FFT-RPCA-SVM method, FFT-BP, FFT-SVM and FFT-PCA-SVM are used in the experiment. The testing samples are randomly selected with different sizes. Each method is running 50 times for each test data set. The average fault diagnosis results of these methods are shown in Table 4.

According to Table 4, the average diagnostic accuracy rate of FFT-BP neural network is around 70%, and the algorithm's average running time is the longest. Although FFT-SVM has similar average diagnostic accuracy rate as that of FFT-RPCA-SVM method, its average running time is much longer than that of FFT-RPCA-SVM's. FFT-PCA-SVM is better than FFT-SVM in diagnostic accuracy and average running time. With less PCs, the diagnostic accuracy of FFT-PCA-SVM comes down. The main reason is that RPCA is used to extract the key features of signal. So, the first PCs can represent better the whole data. Compared with other three methods, FFT-RPCA-SVM is able to greatly reduce the calculation time, and improve the diagnostic accuracy. It is clear that the FFT-RPCA-SVM method is more performant than the other compared methods from the experimental results.

6. Conclusion

In order to improve the accuracy of fault diagnosis and accelerate the operation speed for high-voltage and high-power systems, a new fault diagnosis method based on FFT-RPCA-SVM is proposed for CHMLIS in this paper. By analyzing the output phase voltage and current signals of CHMLIS, the proposed method selects output voltage signals as the fault characteristic signals. The main steps of this method are as follows. Firstly, the sampled data are preprocessed based on FFT to reduce the number of significant data. Secondly, RPCA is used to further reduce the dimension of original feature data, extract main features of complex data. Then, SVM is adopted for its high classification accuracy and strong generalization ability. Finally the cascaded H-bridge multi-level inverter fault diagnosis experimental platform based on dSPACE1104 has been built. Compared with FFT-BP and FFT-SVM, the simulated and experimental results show that the proposed fault diagnosis method is superior to traditional methods. The proposed FFT-RPCA-SVM method has better fault diagnostic accuracy and faster running speed, which will directly reduce the electrical equipment's operating time and extend the working life of the equipment under abnormal conditions.

Acknowledgement

This paper was supported by the projects of NSFC (61203089, 61304186 and 61403229) and Innovation Key Project of Shanghai Municipal Education Commission (14ZZ141). The authors thank the anonymous reviewers for their useful comments and suggestions.

References

[1] Estima JO, Cardoso AJM. A new approach for real-time multiple open-circuit fault diagnosis in voltage-source inverters. IEEE Trans Ind Appl 2011;47(6):2487–94.
[2] Wang T, Xu H, Han J, Benbouzid M. Cascaded H-bridge multilevel inverter system fault diagnosis using a PCA and multi-class relevance vector machine approach. IEEE Transactions on Power Electronics 2015;30(12):7006–18.
[3] Lezana P, Pou J, Meynard TA, Rodriguez J, Ceballos S, Richardeau F. Survey on fault operation on multilevel inverters. IEEE Trans Ind Electron 2010;57(7):2207–18.
[4] Tabbache B, Benbouzid M, Kheloui A. An improved fault-tolerant control scheme for PWM inverter-fed induction motor-based EVs. ISA Trans 2013;52(6):862–9.
[5] Alavi M, Wang Danwei, Luo Ming. Short-circuit fault diagnosis for three-phase inverters based on voltage-space patterns. IEEE Trans Ind Electron 2014;61(10):5558–69.
[6] Carnielutti F, Pinheiro H, Rech C. Generalized carrier-based modulation strategy for cascaded multilevel converters operating under fault conditions. IEEE Trans Ind Electron 2012;59(2):679–89.
[7] Dominic D Arun, Chelliah Thanga Raj. Analysis of field-oriented controlled induction motor drives under sensor faults and an overview of sensorless schemes. ISA Trans 2014;53(5):1680–94.
[8] Adam GP, Ahmed KH, Finney SJ, Bell K, Williams BW. New breed of network fault-tolerant voltage-source-converter HVDC transmission system. IEEE Trans Power Syst 2013;28(1):335–46.
[9] Song Wenchao, Huang AQ. Fault-tolerant design and control strategy for cascaded H-Bridge multilevel converter-based STATCOM. IEEE Trans Ind Electron 2010;57(8):2700–8.
[10] Choi Ui-Min, Lee Kyo-Beum, Blaabjerg F. Diagnosis and tolerant strategy of an open-switch fault for t-type three-level inverter systems. IEEE Trans Ind Appl 2014;50(1):495–508.
[11] Shao Shuai, Wheeler PW, Clare JC, Watson AJ. Fault detection for modular multilevel converters based on sliding mode observer. IEEE Trans Power Electron 2013;28(11):4867–72.

[12] Jung Shin-Myung, Park Jin-Sik, Kim Hag-Wone, Cho Kwan-Yuhl, Youn Myung-Joong. An MRAS-based diagnosis of open-circuit fault in PWM voltage-source inverters for PM synchronous motor drive systems. IEEE Trans Power Electron 2013;28(5):2514–26.
[13] Nie Songsong, Pei Xuejun, Chen Yu, Kang Yong. Fault diagnosis of PWM DC–DC converters based on magnetic component voltages equation. IEEE Trans Power Electron 2014;29(9):4978–88.
[14] Salem Samira Ben, Bacha Khmais, Chaari Abdelkader. Support vector machine based decision for mechanical fault condition monitoring in induction motor using an advanced Hilbert-Park transform. ISA Trans 2012;51(5):566–72.
[15] Mourad E, Nayak A. Comparison-based system-level fault diagnosis: a neural network approach. IEEE Trans Parallel Distrib Syst 2012;23(6):1047–59.
[16] Alkaya Alkan, Eker Ilyas. Variance sensitive adaptive threshold-based PCA method for fault detection with experimental application. ISA Trans 2011;50(2):287–302.
[17] Berriri H, Naouar MW, Slama-Belkhodja I. Easy and fast sensor fault detection and isolation algorithm for electrical drives. IEEE Trans Power Electron 2012;27(2):490–9.
[18] Mozaffari-Kermani M, Azarderakhsh R. Efficient fault diagnosis schemes for reliable lightweight cryptographic ISO/IEC standard CLEFIA benchmarked on ASIC and FPGA. IEEE Trans Ind Electron 2013;60(12):5925–32.
[19] Ye Fangming, Zhang Zhaobo, Chakrabarty K, Gu Xinli. Board-level functional fault diagnosis using multikernel support vector machines and incremental learning. IEEE Trans Comput-Aided Des Integr Circuits Syst 2014;33(2):279–90.
[20] Peng HX, Chen XG, Xu W. Application of PCA feature extraction and SVM Multi-classification sensor fault diagnosis. J Data Acquis Process 2010;25(6):111–6.
[21] Song GM, Wang HJ, Liu H, Jiang SY. Analog circuit fault diagnosis using lifting wavelet transform and SVM. J Electron Meas Instrum 2010;24(7):17–22.
[22] Ranaee V, Ebrahimzadeh A, Ghaderi Reza. Application of the PSO-SVM model for recognition of control chart patterns. ISA Trans 2010;49(4):577–86.
[23] Li Chaoshun, Zhou Jianzhong. Semi-supervised weighted kernel clustering based on gravitational search for fault diagnosis. ISA Trans 2014;53(5):1534–43.
[24] Marques Jorge F, Estima Jorge O, Gameiro Natália S, Marques Cardoso AJ. A new diagnostic technique for real-time diagnosis of power converter faults in switched reluctance motor drives. IEEE Trans Ind Appl 2014;50(3):1854–60.
[25] Ben Smida M, Ben Ammar F. Modeling and DBC-PSC-PWM control of a three-phase flying-capacitor stacked multilevel voltage source inverter. IEEE Trans Ind Electron 2010;57(7):2231–9.
[26] Chen Q, Wang QJ, Li GL, Jiang WD. Analysis and comparison of power losses in 3L NPC inverter with SHPWM control. Electr Mach Syst 2012;15(7):1–5.
[27] Bodo N, Levi E, Jones M. Investigation of carrier-based PWM techniques for a five-phase open-end winding drive topology. IEEE Trans Ind Electron 2013;60(5):2054–65.
[28] Wang Rui, Zhao Jin, Liu Yang. A comprehensive investigation of four-switch three-phase voltage source inverter based on double fourier integral analysis. IEEE Trans Power Electron 2011;26(10):2774–87.
[29] Tian-zhen Wang, Tian-hao Tang, Cheng-lin Wen, Hong-qiong Huang. Relative principal component analysis algorithm and its application in fault detection. J Syst Simul 2007;19(13):2889–94.
[30] Hu Zhikun, Chen Zhiwen, Gui Weihua, Jiang Bin. Adaptive PCA based fault diagnosis scheme in imperial smelting process. ISA Trans 2014;53(5):1446–55.
[31] Feng GH. Parameter optimizing for support vector machines classification. Comput Eng Appl 2011;47:123–4.

Please cite this article as: Wang T, et al. Fault diagnosis method based on FFT-RPCA-SVM for Cascaded-Multilevel Inverter. ISA Transactions (2015), http://dx.doi.org/10.1016/j.isatra.2015.11.018